Momentum Amplituhedron for $\mathcal{N}=6$ Chern-Simons-Matter Theory: Scattering Amplitudes from Configurations of Points in Minkowski Space

Tomasz Łukowski* and Jonah Stalknecht†
Department of Physics, Astronomy and Mathematics, University of Hertfordshire, AL10 9AB Hatfield, Hertfordshire, United Kingdom

(Received 17 July 2023; accepted 20 September 2023; published 17 October 2023)

In this Letter, we define the Aharony-Bergman-Jafferis-Maldacena loop momentum amplituhedron, which is a geometry encoding Aharony-Bergman-Jafferis-Maldacena planar tree-level amplitudes and loop integrands in the three-dimensional spinor helicity space. Translating it to the space of dual momenta produces a remarkably simple geometry given by configurations of spacelike separated off-shell momenta living inside a curvy polytope defined by momenta of scattered particles. We conjecture that the canonical differential form on this space gives amplitude integrands, and we provide a new formula for all one-loop n-particle integrands in the positive branch. For higher loop orders, we utilize the causal structure of configurations of points in Minkowski space to explain the singularity structure for known results at two loops.

DOI: 10.1103/PhysRevLett.131.161601

Introduction.—Recent years have seen remarkable progress in applying positive geometries [1] to the problem of finding scattering amplitudes. The most famous example is the amplituhedron [2–20], which describes scattering amplitudes and loop integrands in planar $\mathcal{N}=4$ super Yang-Mills (SYM) in four-dimensional momentum twistor space, that was based on previous works on positive Grassmannians [21–23]. More relevant to our work, the momentum amplituhedron [24–29] describes tree-level amplitudes in $\mathcal{N}=4$ SYM directly in four-dimensional spinor helicity space, and was recently extended to include loop integrands [30]. In past years, there has been a continued interest in extending these ideas to Aharony-Bergman-Jafferis-Maldacena (ABJM) theory, which has a similar Grassmannian formulation [31–35]. This led to the discovery of the ABJM momentum amplituhedron [36–38], which describes tree-level ABJM amplitudes in three-dimensional spinor helicity space. Most recently, by considering the reduction of the kinematics from the four-dimensional space of massless momenta to three dimensions, the ABJM amplituhedron $\mathcal{W}_n^{(L)}$ was defined [39–42] in the three-dimensional momentum twistor space. This geometry encodes planar tree-level amplitudes $A_n^{(0)}$ and loop integrands $A_n^{(L)}$ in its canonical differential form. Importantly, it was conjectured in [42] that the L-loop integrands can be explicitly obtained from the ABJM amplituhedron by subdividing it into smaller pieces that are cartesian products of tree-level geometry ($\mathcal{C}_m$) times the L-loop geometry ($\mathcal{L}_m^{(L)}$)

$$\mathcal{W}_n^{(L)} = \cup_m \mathcal{C}_m \times \mathcal{L}_m^{(L)}, \tag{1}$$

where $\mathcal{C}_m$ are maximal intersections of Britto-Cachazo-Feng-Witten cells at tree level termed "chambers." For a given chamber, the loop geometry is the same, and can be thought of as a fibration of the loop amplituhedron over the tree one.

In this Letter we define a close cousin to the ABJM amplituhedron we termed the "ABJM momentum amplituhedron" $\mathcal{A}_n^{(L)}$, that lives directly in the three-dimensional spinor helicity space. To do that, we utilize the map used in the recently conjectured construction of the loop momentum amplituhedron for $\mathcal{N}=4$ SYM [30]. This will define a geometry whose differential form is the integrand for the so-called "positive branch" of the theory. Importantly, the geometry that we obtain is remarkably basic when depicted in the space of dual momenta in three-dimensional Minkowski space. In particular, for a given tree-level configuration of points in $\mathcal{C}_m$, the loop geometry is a subset of the Cartesian product of L curvy versions of simple polytopes [43] we denote $\Delta_n^{(m)}$. Remarkably, at one loop the ABJM loop momentum amplituhedron in a given chamber *is* the curvy polytope $\Delta_n^{(m)}$, and it is straightforward to find its canonical form. For each chamber one can easily identify vertices of $\Delta_n^{(m)}$ and therefore find a general form of all one-loop integrands $A_n^{(1)}$ in the positive branch for scattering amplitudes with $n=2k$ particles:

$$A_n^{(1)} = \sum_{(T_1,T_2)\in\mathcal{T}^o\times\mathcal{T}^e} \Omega^{(0)}_{T_1,T_2} \wedge \Omega^{(1)}_{T_1,T_2}. \tag{2}$$

Here, $\Omega^{(0)}_{T_1,T_2}$ is the tree-level canonical form for a given chamber that we labeled by a pair of triangulations (T_1, T_2) of two k-gons formed of odd and even particle labels. The one-loop differential form $\Omega^{(1)}_{T_1,T_2}$ associated with the chamber (T_1, T_2) takes the form

$$\Omega^{(1)}_{T_1,T_2} = \sum_{a=1}^{n} (-1)^a \omega_{a-1,a,a+1} + \sum_{(a,b,c)\in T_1} \omega^{+}_{abc} - \sum_{(a,b,c)\in T_2} \omega^{-}_{abc},$$

and we present its explicit expression later. Results for other branches can be obtained from (2) by parity operations defined in [42].

For higher loops, the ABJM momentum amplituhedron $\mathcal{A}_n^{(L)}$ is specified by configurations of L points inside $\Delta_n^{(m)}$ that are spacelike separated from each other. By studying such configurations of points, we are able to give a simple explanation for the structure of the answer for the two-loop integrands known for $n = 4$ [45,46], $n = 6$ [47], and $n = 8$ [48]. To do that, we will utilize the notion of negative geometries [49] and use the causal structure of the three-dimensional Minkowski space.

This Letter is organized as follows: we start by recalling basic facts about three-dimensional Minkowski space that will set the stage for next sections. Then, we study configurations of dual momenta that originate from the definition of the tree-level ABJM momentum amplituhedron that will allow us to define the curvy polytopes $\Delta_n^{(m)}$. We follow by defining the ABJM momentum amplituhedron at loop level, and detailing its structure at one loop. In particular, we provide the explicit formula for one-loop integrands in the positive branch for all multiplicities. The final section focuses on the two-loop geometry. We conclude the Letter with some open questions arising from our construction.

Three-dimensional Minkowski space.—We will work in the three-dimensional Minkowski space $\mathcal{M}$ with signature $(+,-,-)$. Scattering data for n-particle scattering in ABJM is encoded in a set of $n = 2k$ three-dimensional on-shell momenta p_a^μ, $a = 1,\ldots,2k$, $\mu = 0, 1, 2$, with $(p_a)^2 = 0$. We assume that particles with odd labels are outgoing and the ones with even labels are incoming. This leads to the following momentum conservation:

$$\sum_{a \text{ odd}} p_a^\mu - \sum_{a \text{ even}} p_a^\mu = 0. \tag{3}$$

In planar theory, this data can be equivalently encoded using dual coordinates,

$$p_a^\mu =: x_{a+1}^\mu - x_a^\mu, \tag{4}$$

that define a null polygon in Minkowski space. For convenience, we choose $x_1 = 0$. This allows us to invert relation (4) to get

$$x_b = \sum_{a=1}^{b-1} (-1)^a p_a. \tag{5}$$

We denote by $\mathcal{I}_x = \{y \in \mathcal{M} : (x-y)^2 = 0\}$ the light cone of point x.

The on-shell condition $p^2 = 0$ can be resolved by introducing three-dimensional spinor helicity variables (see, e.g., [50] for a review) and writing

$$p^{\alpha\beta} = \begin{pmatrix} -p^0 + p^2 & p^1 \\ p^1 & -p^0 - p^2 \end{pmatrix} =: \lambda^\alpha \lambda^\beta. \tag{6}$$

Scattering amplitudes are invariant under the action of the Lorentz group $SL(2)$ on λ and therefore a point in the kinematic space is an element of the orthogonal Grassmannian $\lambda \in OG(2,2k) =: \mathcal{K}_{2k}$, where orthogonality is defined with respect to $\eta = \mathrm{diag}(+,-,\ldots,+,-)$. In the following, we will repeatedly use the spinor brackets $\langle ab\rangle := \lambda_a^1\lambda_b^2 - \lambda_a^2\lambda_b^1$.

Tree-level momentum amplituhedron.—Following [36,37], the tree-level ABJM momentum amplituhedron $\mathcal{A}_{2k}^{(0)} = \phi_\Lambda[OG_+(k,2k)]$ is a subset of the kinematic space $\mathcal{K}_{2k}$, which is the image of the positive orthogonal Grassmannian $OG_+(k,2k)$ through the map

$$\begin{aligned} \phi_\Lambda :\ & OG_+(k,2k) \to OG(2,2k) \\ & C \mapsto \lambda = (C\cdot\eta\cdot\Lambda)^\perp \cdot \Lambda, \end{aligned} \tag{7}$$

where $\Lambda \in M(k+2,2k)$ is a fixed matrix [51]. To get the desired geometry, in this Letter we slightly modify the original definition and demand that the matrix Λ is such that the image contains points satisfying the following sign-flip pattern: $\langle ii+1\rangle > 0$ for all $i = 1,\ldots,n$; the sequence $\{\langle 12\rangle, \langle 13\rangle, \ldots, \langle 1n\rangle\}$ has $k-2$ sign flips and all planar Mandelstams are negative. We found that taking a generic twisted positive matrix Λ, i.e., $\Lambda\cdot\eta$ has all maximal minors positive, leads to the correct sign-flip pattern.

Importantly, for every point $\lambda \in \mathcal{A}_{2k}^{(0)}$, when translated to the dual space we get a configuration of dual points x_a, $a = 1,\ldots,n$ forming a null polygonal loop, that satisfy the conditions

$$(x_a - x_b)^2 < 0, \quad \text{for } |a-b| > 1, \tag{8}$$

and all even-indexed points are in the future of their (null-separated) odd-indexed two neighbors.

These configurations of points x_a have a very interesting and intricate structure. In particular, for any three generic points x_a, x_b, and x_c that are not neighbors, we find

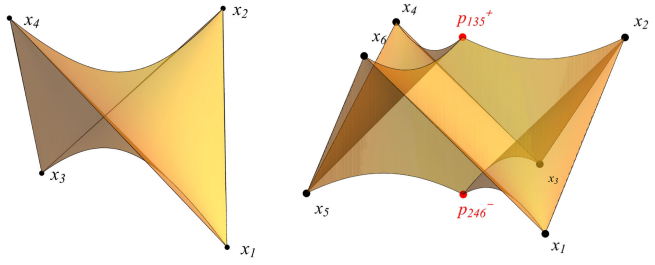

FIG. 1. The region Δ_n that is the compact part of the set of all points that are spacelike separated from x_a for $n = 4$ and $n = 6$.

two points in the intersection of their light cones $\mathcal{I}_{x_a} \cap \mathcal{I}_{x_b} \cap \mathcal{I}_{x_c}$, one in the future of points (x_a, x_b, x_c), and one in the past. We denote the future (past) point as p^+_{abc} (p^-_{abc}). Motivated by our future considerations, let us define the region of the Minkowski space,

$$\mathcal{K}^{\leq 0}_{x_a} := \{x \in \mathcal{M} : (x - x_a)^2 \leq 0 \quad \text{for } a = 1, \ldots, n\}, \quad (9)$$

containing all points that are spacelike (or lightlike) separated from all x_a. This region is nonempty since $x_a \in \mathcal{K}^{\leq 0}_{x_a}$ for all $a = 1, \ldots, n$. Moreover, it can be naturally divided into two pieces: a compact one that we denote $\Delta_n(x_a)$ and a noncompact one $\bar{\Delta}_n(x_a)$. We depict the compact region for $n = 4$ and $n = 6$ in Fig. 1. It is easy to see that the region $\Delta_4(x_a)$ is a curvy version of a tetrahedron, while $\Delta_6(x_a)$ is a curvy version of a cube. The latter has two vertices coming from triple intersections of light cones, p^+_{135} and p^-_{246}, in addition to the six vertices x_i. For higher n, the shape of $\Delta_n(x_a)$ is more involved and starts to depend on the details of the configuration of xs. For example, for $n = 8$ there are four distinct geometries $\Delta^{(m)}_8(x_a)$, each of them contains eight vertices x_a together with triple intersections of light cones:

$$\begin{aligned}
\mathcal{V}[\Delta^{(1)}_8(x_a)] &= \{x_a, p^+_{135}, p^+_{157}, p^-_{246}, p^-_{268}\},\\
\mathcal{V}[\Delta^{(2)}_8(x_a)] &= \{x_a, p^+_{137}, p^+_{357}, p^-_{246}, p^-_{268}\},\\
\mathcal{V}[\Delta^{(3)}_8(x_a)] &= \{x_a, p^+_{135}, p^+_{157}, p^-_{248}, p^-_{468}\},\\
\mathcal{V}[\Delta^{(4)}_8(x_a)] &= \{x_a, p^+_{137}, p^+_{357}, p^-_{248}, p^-_{468}\}.
\end{aligned}$$

These four cases exactly correspond to the four chambers for $n = 8$ in [42]! One notices that the labels of the intersecting cones for each chamber can be thought of as products of triangulations of two 4-gons: one formed of odd labels, and one formed of even labels. This pattern continues for higher n. We found that there are exactly C^2_{k-2} different geometries $\Delta^{(m)}_n$ for $n = 2k$ particles, where C_p is the pth Catalan number. All these geometries have n vertices corresponding to x_a together with exactly $(k-2)$ triple intersections of light cones of points with odd labels, and $(k-2)$ intersections with even labels. The geometry changes at nongeneric configurations of points x_a, where an intersection of four light cones is possible, corresponding to a bistellar flip in one of the aforementioned triangulations. All curvy polytopes $\Delta^{(m)}_n$ are *simple*, meaning that each vertex has exactly three edges originating from it.

We note that the two triangulations of k-gons are more than just a mnemonic to distinguish distinct geometries: they in fact provide part of the skeleton of the dual geometry of $\Delta^{(m)}_n$! The fact that the facets of this dual are all triangles is equivalent to the statement that polytopes $\Delta^{(m)}_n$ are simple. The triangles with vertices (a, b, c) in the dual correspond to vertices p_{abc} of $\Delta^{(m)}_n$. Since the dual of a triangulation of a k-gon is a planar tree Feynman diagram for k particles, the skeleton of our geometry is that of a null polygon between points x_a, with two distinct Feynman diagrams drawn between the odd and even points, where different choices of Feynman diagrams label different chambers. Therefore, distinct $\Delta^{(m)}_n$ correspond to all pairs of two planar tree Feynman diagrams for k particles.

Loop-level momentum amplituhedron.—Given a fixed tree-level configuration $\lambda \in \mathcal{A}^{(0)}_n$, we will define the ABJM loop momentum amplituhedron using the map

$$\begin{aligned}
\Phi_\lambda :\ & G(2, 2k)^L \to GL(2)^L\\
& (D_1, \ldots, D_L) \mapsto (\ell_1, \ldots, \ell_L)
\end{aligned} \quad (10)$$

that was introduced for $\mathcal{N} = 4$ SYM in [30]. It is defined by

$$\ell_l = \frac{\sum_{a<b} (ab)_{D_l} \ell^\star_{ab}}{\sum_{a<b} (ab)_{D_l} \langle ab \rangle}, \quad (11)$$

where the matrix D_l is an element of Grassmannian space $G(2, 2k)$ and $(ab)_{D_l}$ are 2×2 minors of the matrix D_l. Moreover, we define

$$\ell^\star_{ab} = \sum_{c=b+1}^{n} (-1)^c \lambda_a \langle bc \rangle \lambda_c - \sum_{c=a+1}^{n} (-1)^c \lambda_b \langle ac \rangle \lambda_c. \quad (12)$$

The image $\ell_l = \Phi_\lambda(D_l)$ is generically not a symmetric matrix, and therefore in order to adapt this construction to the ABJM theory, we need to restrict to a subsets of matrices D_l that result in three dimensional off-shell momenta. This imposes additional constraints on D_l, which correspond to the symplectic condition described in [42].

We define the loop momentum amplituhedron $\mathcal{A}^{(L)}_{2k}$ as the image of a particular subset $\mathcal{D}_L \subset G(2, 2k) \times \ldots \times G(2, 2k)$ obtained as follows. We take a matrix $C \in OG_+(k)$ such that $\lambda = \phi_\Lambda(C)$ and construct its T-dual version $\check{C}$ (see [52]). Then we say that $(D_1, \ldots, D_L) \in \mathcal{D}_L$ if

the matrices $(\check{C}, D_{l_1}, \ldots, D_{l_p})$ are positive for all subsets $\{l_1, \ldots, l_p\} \subset \{1, \ldots, L\}$. Finally, we can define

$$\mathcal{A}_{2k}^{(L)} = \Phi_\lambda(\mathcal{D}_L). \tag{13}$$

One loop.—We start our exploration of the loop momentum amplituhedron by examining the one-loop geometry $\mathcal{A}_{2k}^{(1)}$, which is relatively basic. One straightforward fact that can be derived from definition (10) is that $\mathcal{A}_{2k}^{(1)} \subset \mathcal{K}_{x_a}^{\leq 0}$, which means that all point $\ell \equiv x \in \mathcal{A}_{2k}^{(1)}$ are spacelike separated from all points x_a. What is far less obvious is the fact that all points of the loop momentum amplituhedron sit in the compact part $\Delta_{2k}(x_a)$ of $\mathcal{K}_{x_a}^{\leq 0}$. We have sampled many random points in the image of (13) for $n \leq 10$ to confirm that they are actually equal:

$$\mathcal{A}_{2k}^{(1)} = \Delta_{2k}^{(m)}, \tag{14}$$

where the geometry depends on the choice of tree-level λ. Most importantly, for all points λ in the same chamber, the loop geometry $\mathcal{A}_{2k}^{(1)}$ looks the same, confirming that the geometry factorizes as in (1).

Knowing the geometry, we can find its canonical differential form. From the factorization property, we immediately get that

$$A_n^{(1)} = \sum_m \Omega_{n,m}^{(0)} \wedge \Omega_{n,m}^{(1)}, \tag{15}$$

where $\Omega_{n,m}^{(0)}$ is the tree-level form associated to the chamber C_m. In the following we will derive explicit expressions for $\Omega_{n,m}^{(1)} = \Omega(\Delta_{2k}^{(m)})$. Since $\Delta_{2k}^{(m)}$ is just a curvy version of a simple polytope in three dimensions, the canonical form should naively be just the sum over vertices of the d log forms for all facets that meet at that vertex

$$\Omega_{\text{naive}}[\Delta_{2k}^{(m)}] = \sum_{(abc) \in \mathcal{V}[\Delta_{2k}^{(m)}]} \sigma_{abc} \omega_{abc}, \tag{16}$$

where

$$\omega_{abc} = d\log(x - x_a)^2 \wedge d\log(x - x_b)^2 \wedge d\log(x - x_c)^2.$$

The signs σ_{abc} can be found by demanding that the form is projective, see [53]. We emphasize that the differential forms ω_{abc} separately are not dual conformally invariant; however, the final answer (16) is. The difference in our case compared to the story of simple polytopes is that the differential form (16) also has nonvanishing residues at points outside of $\Delta_{2k}^{(m)}$. More precisely, it has a nonzero residue at all points $p_{abc}^{\pm}$, while only one of them is a vertex of $\Delta_{2k}^{(m)}$. Since

$$\operatorname*{Res}_{x = p_{abc}^{\pm}} \omega_{abc} = 1, \tag{17}$$

we need to find a form that contributes with opposite signs on the two points. The natural candidate is the triangle integrand

$$\begin{aligned}\omega_{abc}^{\triangle} &= \frac{4\sqrt{x_{ab}^2 x_{bc}^2 x_{ac}^2}\, \mathrm{d}^3 x}{(x - x_a)^2 (x - x_b)^2 (x - x_c)^2} \\ &= \pm d\log\frac{(x - x_a)^2}{(x - p_{abc}^{\pm})^2} \wedge d\log\frac{(x - x_b)^2}{(x - p_{abc}^{\pm})^2} \wedge d\log\frac{(x - x_c)^2}{(x - p_{abc}^{\pm})^2},\end{aligned} \tag{18}$$

for which

$$\operatorname*{Res}_{x = p_{abc}^{\pm}} \omega_{abc}^{\triangle} = \pm 1. \tag{19}$$

Therefore, the form that is supported only on $\Delta_{2k}^{(m)}$ is

$$\Omega(\Delta_{2k}^{(m)}) = \sum_{(abc) \in \mathcal{V}[\Delta_{2k}^{(m)}]} \sigma_{abc} \omega_{abc}^{\pm} = \sum_{(abc)} \sigma_{abc} (\omega_{abc} \pm \omega_{abc}^{\triangle}),$$

where the relative sign in the bracket depends on which solution of the triple intersection is a vertex of the geometry. Performing case-by-case studies, one finds that all intersections with even labels have negative sign, while all with odd labels positive sign. We note that the light cones that meet at vertices x_a are given by $(x - x_{a-1})^2 = 0$, $(x - x_a)^2 = 0$, and $(x - x_{a+1})^2 = 0$, and since $\omega_{a-1aa+1}^{\triangle} = 0$ these vertices only contribute $\omega_{a-1aa+1}$. We notice that the form $\Omega[\Delta_{2k}^{(m)}]$ has a residue of 2 at $p_{abc}^{\pm}$, whereas there is a residue of 1 at vertices x_a. This is a necessary feature to ensure projective invariance, and it leads to the correct integrand. The generalization of positive geometries that allows for these type of residues has been recently introduced in [20] in the context of the loop amplituhedron. Therefore, we conjecture that the one-loop ABJM integrand for the positive branch for any $n = 2k$ is (2). The formula agrees with the one provided in [42] for $n = 4, 6, 8, 10$ [54].

As argued in [42], the complete $2k$-point ABJM integrand is given by a sum over 2^{k-2} different branches. While our current construction of the geometry gives the integrand only for the positive branch, the integrands for other branches can be obtained from (2) by making use of the parity operations introduced in [42]. These effectively interchange certain $p_{abc}^{+} \leftrightarrow p_{abc}^{-}$, while keeping all points x_a unchanged. Therefore, we can think of other branches as having exactly the same shape $\Delta_{2k}^{(m)}$ as the positive branch, but with some of the triple intersection points swapped. It is clear that such a parity operation will only flip the signs of the corresponding triangle integrands, while leaving the rest of the form unchanged. Therefore, if one is able to classify all parity operations for given n, the full amplitude can be derived from our geometric construction by summing over these relabeled geometries.

More loops.—In this section we will have a first look at implications of our construction for the L-loop problem for $L > 1$. In this case, each off-shell loop momentum ℓ_l is spacelike separated from all points x_a and therefore sits inside $\Delta_{2k}^{(m)}$. However, we also need to impose mutual positivity constraints that translate into the requirement that every pair of loop momenta is spacelike separated $(\ell_{l_1} - \ell_{l_2})^2 < 0$ for all $l_1, l_2 = 1, \ldots, L$.

This is particularly simple for $n = 4$ at two loops, where for a fixed position of momentum ℓ_1, the geometry accessible to the momentum ℓ_2, depicted in Fig. 2(a), does not depend on the position of ℓ_1. We are therefore interested in the region inside Δ_4 that sits outside the light cone of ℓ_1. Importantly, the latter intersects the light cones of points x_1 and x_3 in the future and the light cones of points x_2 and x_4 in the past. It is not obvious how to directly find the canonical differential form of this region. We will however circumvent this problem by considering negative geometries; see [39,49]. It is clear that

$$\mathcal{A}_4^{(2)} \cup \mathcal{R}_4 = \mathcal{A}_4^{(1)} \times \mathcal{A}_4^{(1)}, \tag{20}$$

where $\mathcal{R}_4 = \{(\ell_1, \ell_2) \in \Delta_4 \times \Delta_4 \colon (\ell_1 - \ell_2)^2 > 0\}$. This region further decomposes into $\mathcal{R}_4 = \mathcal{R}_{4,\ell_1 \prec \ell_2} \cup \mathcal{R}_{4,\ell_1 \succ \ell_2}$, where $\mathcal{R}_{4,\ell_1 \prec \ell_2}$ ($\mathcal{R}_{4,\ell_1 \prec \ell_2}$) contains all points for which ℓ_1 is in the past (future) of ℓ_2. The boundary structure of these two regions is significantly simpler then the one of $\mathcal{A}_4^{(2)}$; see Fig. 2(b). In particular, the only boundaries accessible by momentum ℓ_1 are $(\ell_1 - \ell_2)^2 = 0$, $(\ell_1 - x_2)^2 = 0$, and $(\ell_1 - x_4)^2 = 0$ $[(\ell_1 - \ell_2)^2 = 0, \quad (\ell_1 - x_1)^2 = 0, \quad \text{and} \quad (\ell_1 - x_3)^2 = 0]$. By comparing with known results, there is a natural differential form that we can associate to each of these regions:

$$\Omega(\mathcal{R}_{4,\ell_1 \prec \ell_2}) = \frac{x_{13}^2 x_{24}^2 d^3\ell_1 \wedge d^3\ell_2}{(\ell_1 - x_2)^2(\ell_1 - x_4)^2(\ell_1 - \ell_2)^2(\ell_2 - x_1)^2(\ell_2 - x_3)^2}$$

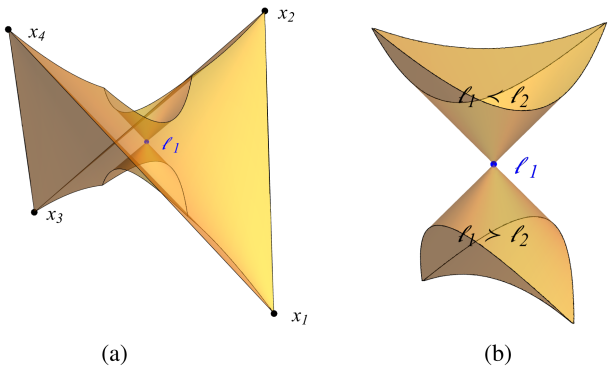

FIG. 2. The positive (a) and negative (b) part of the geometry for $n = 4$ for fixed ℓ_1.

and $\Omega(\mathcal{R}_{4,\ell_1 \succ \ell_2}) = \Omega(\mathcal{R}_{4,\ell_1 \prec \ell_2})|_{\ell_1 \leftrightarrow \ell_2}$. Therefore, the two-loop integrand is given by

$$\Omega_4^{(2)} = \Omega_1^{(1)}(\ell_1) \wedge \Omega_1^{(1)}(\ell_2) - \Omega(\mathcal{R}_{4,\ell_1 \prec \ell_2}) - \Omega(\mathcal{R}_{4,\ell_1 \succ \ell_2}). \tag{21}$$

This agrees with [45].

For higher number of points at two loops, we observe that, when going to negative geometries, we can again define two regions, $\mathcal{R}_{n,\ell_1 \prec \ell_2}$ and $\mathcal{R}_{n,\ell_1 \succ \ell_2}$, where loop momenta are timelike separated and time-ordered. Unlike for $n = 4$, we get different regions for ℓ_2 depending on the position of ℓ_1. However, there is a simple classification of all these regions. We focus first on $\mathcal{R}_{6,\ell_1 \prec \ell_2}$ and notice that for fixed ℓ_1 the only boundaries for momentum ℓ_2 are at $(\ell_1 - \ell_2)^2 = 0$ and at the light cones of points x_a that intersect the light cone of ℓ_1 in the future. There are four possibilities:

$$\{\mathcal{I}_{\ell_1} \cap \mathcal{I}_{x_1} \neq \emptyset, \mathcal{I}_{\ell_1} \cap \mathcal{I}_{x_3} \neq \emptyset\}, \tag{22}$$

$$\{\mathcal{I}_{\ell_1} \cap \mathcal{I}_{x_1} \neq \emptyset, \mathcal{I}_{\ell_1} \cap \mathcal{I}_{x_5} \neq \emptyset\}, \tag{23}$$

$$\{\mathcal{I}_{\ell_1} \cap \mathcal{I}_{x_3} \neq \emptyset, \mathcal{I}_{\ell_1} \cap \mathcal{I}_{x_5} \neq \emptyset\}, \tag{24}$$

$$\{\mathcal{I}_{\ell_1} \cap \mathcal{I}_{x_1} \neq \emptyset, \mathcal{I}_{\ell_1} \cap \mathcal{I}_{x_3} \neq \emptyset, \mathcal{I}_{\ell_1} \cap \mathcal{I}_{x_5} \neq \emptyset\}, \tag{25}$$

as depicted in Fig. 3. Similar analysis holds true for boundaries for ℓ_1 when ℓ_2 is fixed: the four possibilities are $\{2,4\}$, $\{2,6\}$, $\{4,6\}$ or $\{2,4,6\}$. We found that there are 13 allowed regions in this geometry [notice that region $(\{2,4\}, \{1,5\})$ and its two cyclic rotations are not allowed], which correspond to the bipartite graphs in [42]. Therefore, it should be possible to rewrite the answer found there such that each term matches one of these 13 regions. Similar structure is also present in the $n = 8$ two-loop answer, and it naturally follows from our construction, since it reflects which light cones intersects $\mathcal{I}_{\ell_1}$ and $\mathcal{I}_{\ell_2}$ in the past and future. At the moment we do not have a good understanding of how to associate differential forms to this regions and leave it for future work.

Finally, by moving to higher loop orders, one can use negative geometries and study configurations of loop

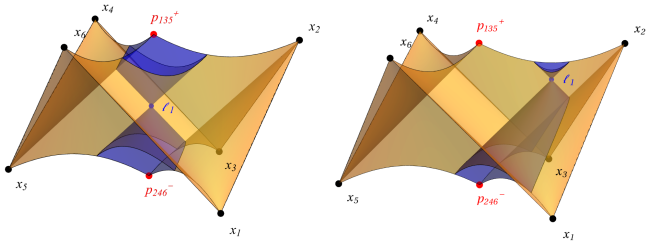

FIG. 3. Two of the 13 possible regions in the two-loop geometry for fixed position of ℓ_1 for $n = 6$.

momenta inside the region $\Delta_n^{(m)}$ that are (partially) time-ordered in three-dimensional Minkowski space, as suggested in [39]. Our construction provides a simple geometric picture that can be used to organize the calculations based on the causal structure of the corresponding configuration of loop momenta.

Conclusions and outlook.—In this Letter we defined the spinor helicity version of the ABJM amplituhedron and, by translating it to the space of dual momenta, we found a surprisingly simple geometry associated with the causal structure of configurations of points in three-dimensional Minkowski space. This allowed us to find a formula for all integrands at one loop, and shed some light on the structure of the answer at two loops and beyond.

Intriguingly, if we knew nothing about amplituhedra, we could still define $\Delta_n(x_a)$ as a compact region in the Minkowski space that is spacelike separated from a null polygon with n vertices. By studying this region we would rediscover the structure of scattering amplitudes in ABJM theory! However, it is far from obvious why ABJM theory is selected from all possible three-dimensional quantum field theories. Finding the answer to this question might shed light on generalizations of our construction beyond ABJM.

There are many interesting avenues to follow based on this new picture of scattering in ABJM. The most urgent one is to better understand the geometry itself and in particular to provide a constructive way to derive its differential forms. It will be crucial to check whether the structure of the answer that we saw at one loop can be systematically generalized to higher loops, promising all multiplicity answers for ABJM loop integrands.

Finally, the ABJM momentum amplituhedron is a reduction of the momentum amplituhedron in $\mathcal{N}=4$ SYM. A natural question that arises is whether a similar basic geometry lives in the four-dimensional space of dual momenta in (2,2) signature.

The authors would like thank Song He, Yu-tin Huang, and Chia-Kai Kuo for useful discussions on their work. We would like to thank the Dublin Institute for Advances Studies for hosting the workshop "Amplituhedron at 10," which provided the initial motivation for this work.

*Corresponding author: t.lukowski@herts.ac.uk
†Corresponding author: j.stalknecht@herts.ac.uk

[1] N. Arkani-Hamed, Y. Bai, and T. Lam, Positive geometries and canonical forms, J. High Energy Phys. 11 (2017) 039.
[2] N. Arkani-Hamed and J. Trnka, The amplituhedron, J. High Energy Phys. 10 (2014) 030.
[3] N. Arkani-Hamed and J. Trnka, Into the amplituhedron, J. High Energy Phys. 12 (2014) 182.
[4] N. Arkani-Hamed, H. Thomas, and J. Trnka, Unwinding the amplituhedron in binary, J. High Energy Phys. 01 (2018) 016.
[5] S. Franco, D. Galloni, A. Mariotti, and J. Trnka, Anatomy of the amplituhedron, J. High Energy Phys. 03 (2015) 128.
[6] E. Herrmann, C. Langer, J. Trnka, and M. Zheng, Positive geometry, local triangulations, and the dual of the Amplituhedron, J. High Energy Phys. 01 (2021) 035.
[7] L. Ferro, T. Lukowski, A. Orta, and M. Parisi, Towards the amplituhedron volume, J. High Energy Phys. 03 (2016) 014.
[8] L. Ferro, T. Łukowski, and M. Parisi, Amplituhedron meets Jeffrey–Kirwan residue, J. Phys. A **52**, 045201 (2019).
[9] T. Lukowski, R. Moerman, and J. Stalknecht, Pushforwards via scattering equations with applications to positive geometries, J. High Energy Phys. 10 (2022) 003.
[10] T. Lukowski, On the boundaries of the $m=2$ amplituhedron, arXiv:1908.00386.
[11] T. Lukowski, M. Parisi, and L. K. Williams, The positive tropical Grassmannian, the hypersimplex, and the $m=2$ amplituhedron, arXiv:2002.06164.
[12] M. Parisi, M. Sherman-Bennett, and L. Williams, The $m=2$ amplituhedron and the hypersimplex: Signs, clusters, triangulations, Eulerian numbers, arXiv:2104.08254.
[13] S. N. Karp and L. K. Williams, The $m=1$ amplituhedron and cyclic hyperplane arrangements, Int. Math. Res. Not. **5**, 1401 (2019).
[14] S. N. Karp, L. K. Williams, and Y. X. Zhang, Decompositions of amplituhedra, Ann. Inst. H. Poincare D Comb. Phys. Interact. **7**, 303 (2020).
[15] N. Arkani-Hamed, C. Langer, A. Yelleshpur Srikant, and J. Trnka, Deep into the amplituhedron: Amplitude singularities at all loops and legs, Phys. Rev. Lett. **122**, 051601 (2019).
[16] A. Yelleshpur Srikant, Emergent unitarity from the amplituhedron, J. High Energy Phys. 01 (2020) 069.
[17] C. Langer and A. Yelleshpur Srikant, All-loop cuts from the amplituhedron, J. High Energy Phys. 04 (2019) 105.
[18] Y. Bai, S. He, and T. Lam, The amplituhedron and the one-loop Grassmannian measure, J. High Energy Phys. 01 (2016) 112.
[19] R. Kojima, Triangulation of 2-loop MHV amplituhedron from sign flips, J. High Energy Phys. 04 (2019) 085.
[20] G. Dian, P. Heslop, and A. Stewart, Internal boundaries of the loop amplituhedron, SciPost Phys. **15**, 098 (2023).
[21] A. Postnikov, Total positivity, Grassmannians, and networks, arXiv:math/0609764.
[22] N. Arkani-Hamed, F. Cachazo, C. Cheung, and J. Kaplan, A duality for the S matrix, J. High Energy Phys. 03 (2010) 020.
[23] N. Arkani-Hamed, J. L. Bourjaily, F. Cachazo, A. B. Goncharov, A. Postnikov, and J. Trnka, *Grassmannian Geometry of Scattering Amplitudes* (Cambridge University Press, Cambridge, England, 2016).
[24] D. Damgaard, L. Ferro, T. Lukowski, and M. Parisi, The momentum amplituhedron, J. High Energy Phys. 08 (2019) 042.
[25] S. He and C. Zhang, Notes on scattering amplitudes as differential forms, J. High Energy Phys. 10 (2018) 054.
[26] D. Damgaard, L. Ferro, T. Lukowski, and R. Moerman, Kleiss-Kuijf relations from momentum amplituhedron geometry, J. High Energy Phys. 07 (2021) 111.

[27] D. Damgaard, L. Ferro, T. Lukowski, and R. Moerman, Momentum amplituhedron meets kinematic associahedron, J. High Energy Phys. 02 (2021) 041.
[28] L. Ferro, T. Łukowski, and R. Moerman, From momentum amplituhedron boundaries toamplitude singularities and back, J. High Energy Phys. 07 (2020) 201.
[29] T. Lukowski and J. Stalknecht, The hypersimplex canonical forms and the momentum amplituhedron-like logarithmic forms, J. Phys. A **55**, 205202 (2022).
[30] L. Ferro and T. Lukowski, The loop momentum amplituhedron, J. High Energy Phys. 05 (2023) 183.
[31] S. Lee, Yangian invariant scattering amplitudes in supersymmetric Chern-Simons theory, Phys. Rev. Lett. **105**, 151603 (2010).
[32] H. Elvang, Y.-t. Huang, C. Keeler, T. Lam, T. M. Olson, S. B. Roland, and D. E. Speyer, Grassmannians for scattering amplitudes in 4d $\mathcal{N} = 4$ SYM and 3d ABJM, J. High Energy Phys. 12 (2014) 181.
[33] Y.-T. Huang and C. Wen, ABJM amplitudes and the positive orthogonal grassmannian, J. High Energy Phys. 02 (2014) 104.
[34] Y.-t. Huang, C. Wen, and D. Xie, The positive orthogonal Grassmannian and loop amplitudes of ABJM, J. Phys. A **47**, 474008 (2014).
[35] J. Kim and S. Lee, Positroid stratification of orthogonal Grassmannian and ABJM amplitudes, J. High Energy Phys. 09 (2014) 085.
[36] S. He, C.-K. Kuo, and Y.-Q. Zhang, The momentum amplituhedron of SYM and ABJM from twistor-string maps, J. High Energy Phys. 02 (2022) 148.
[37] Y.-t. Huang, R. Kojima, C. Wen, and S.-Q. Zhang, The orthogonal momentum amplituhedron and ABJM amplitudes, J. High Energy Phys. 01 (2022) 141.
[38] T. Lukowski, R. Moerman, and J. Stalknecht, On the geometry of the orthogonal momentum amplituhedron, J. High Energy Phys. 12 (2022) 006.
[39] S. He, C.-K. Kuo, Z. Li, and Y.-Q. Zhang, All-loop four-point Aharony-Bergman-Jafferis-Maldacena amplitudes from dimensional reduction of the amplituhedron, Phys. Rev. Lett. **129**, 221604 (2022).
[40] S. He, C.-K. Kuo, Z. Li, and Y.-Q. Zhang, Emergent unitarity, all-loop cuts and integrations from the ABJM amplituhedron, J. High Energy Phys. 07 (2023) 212.
[41] J. M. Henn, M. Lagares, and S.-Q. Zhang, Integrated negative geometries in ABJM, J. High Energy Phys. 05 (2023) 112.
[42] S. He, Y.-t. Huang, and C.-K. Kuo, The ABJM amplituhedron, arXiv:2306.00951.
[43] These types of "curvy polytopes," where the boundaries are given by nonlinear equations, are also known as "polypols." See [44] for a review on polypols and their relation to positive geometries.
[44] K. Kohn, R. Piene, K. Ranestad, F. Rydell, B. Shapiro, R. Sinn, M.-S. Sorea, and S. Telen, Adjoints and canonical forms of polypols, arXiv:2108.11747.
[45] W.-M. Chen and Y.-t. Huang, Dualities for loop amplitudes of $N = 6$ Chern-Simons matter theory, J. High Energy Phys. 11 (2011) 057.
[46] M. S. Bianchi, M. Leoni, A. Mauri, S. Penati, and A. Santambrogio, Scattering amplitudes/wilson loop duality In ABJM theory, J. High Energy Phys. 01 (2012) 056.
[47] S. Caron-Huot and Y.-t. Huang, The two-loop six-point amplitude in ABJM theory, J. High Energy Phys. 03 (2013) 075.
[48] S. He, Y.-t. Huang, C.-K. Kuo, and Z. Li, The two-loop eight-point amplitude in ABJM theory, J. High Energy Phys. 02 (2023) 065.
[49] N. Arkani-Hamed, J. Henn, and J. Trnka, Nonperturbative negative geometries: Amplitudes at strong coupling and the amplituhedron, J. High Energy Phys. 03 (2022) 108.
[50] H. Elvang and Y.-t. Huang, Scattering amplitudes, arXiv:1308.1697.
[51] We use a modified version of the definition in [36,37] that can be mapped to the original one by the parity duality.
[52] N. Arkani-Hamed, J. Bourjaily, F. Cachazo, and J. Trnka, Unification of residues and Grassmannian dualities, J. High Energy Phys. 01 (2011) 049.
[53] N. Arkani-Hamed, Y. Bai, S. He, and G. Yan, Scattering forms and the positive geometry of kinematics, color and the worldsheet, J. High Energy Phys. 05 (2018) 096.
[54] It would also be interesting to compare our result to the all-multiplicity one-loop formula found in [55] for a subset of component amplitudes.
[55] M. S. Bianchi, M. Leoni, A. Mauri, S. Penati, and A. Santambrogio, One loop amplitudes In ABJM, J. High Energy Phys. 07 (2012) 029.